



This is a repository copy of *Heterogeneous reaction of ClONO₂ with TiO₂ and SiO₂ aerosol particles: implications for stratospheric particle injection for climate engineering*.

White Rose Research Online URL for this paper:
<http://eprints.whiterose.ac.uk/106283/>

Version: Published Version

Article:

Tang, M. J., Keeble, J., Telford, P. J. et al. (9 more authors) (2016) Heterogeneous reaction of ClONO₂ with TiO₂ and SiO₂ aerosol particles: implications for stratospheric particle injection for climate engineering. *Atmospheric Chemistry and Physics Discussions*, 16. pp. 15397-15412. ISSN 1680-7367

<https://doi.org/10.5194/acp-16-15397-2016>

Reuse

This article is distributed under the terms of the Creative Commons Attribution (CC BY) licence. This licence allows you to distribute, remix, tweak, and build upon the work, even commercially, as long as you credit the authors for the original work. More information and the full terms of the licence here:
<https://creativecommons.org/licenses/>

Takedown

If you consider content in White Rose Research Online to be in breach of UK law, please notify us by emailing eprints@whiterose.ac.uk including the URL of the record and the reason for the withdrawal request.



eprints@whiterose.ac.uk
<https://eprints.whiterose.ac.uk/>



Heterogeneous reaction of ClONO₂ with TiO₂ and SiO₂ aerosol particles: implications for stratospheric particle injection for climate engineering

Mingjin Tang^{1,2,7}, James Keeble¹, Paul J. Telford^{1,3}, Francis D. Pope⁴, Peter Braesicke⁵, Paul T. Griffiths^{1,3}, N. Luke Abraham^{1,3}, James McGregor⁶, I. Matt Watson², R. Anthony Cox¹, John A. Pyle^{1,3}, and Markus Kalberer¹

¹Department of Chemistry, University of Cambridge, Cambridge CB2 1EW, UK

²School of Earth Sciences, University of Bristol, Bristol BS8 1RJ, UK

³National Centre for Atmospheric Science, NCAS, Cambridge, UK

⁴School of Geography, Earth and Environmental Sciences, University of Birmingham, Birmingham B15 2TT, UK

⁵IMK-ASF, Karlsruhe Institute of Technology, Karlsruhe, Germany

⁶Department of Chemical and Biological Engineering, University of Sheffield, Sheffield S1 3JD, UK

⁷State Key Laboratory of Organic Geochemistry, Guangzhou Institute of Geochemistry, Chinese Academy of Sciences, Guangzhou 510640, China

Correspondence to: Markus Kalberer (markus.kalberer@atm.ch.cam.ac.uk)

Received: 22 August 2016 – Published in Atmos. Chem. Phys. Discuss.: 23 August 2016

Revised: 19 November 2016 – Accepted: 22 November 2016 – Published: 12 December 2016

Abstract. Deliberate injection of aerosol particles into the stratosphere is a potential climate engineering scheme. Particles injected into the stratosphere would scatter solar radiation back to space, thereby reducing the temperature at the Earth's surface and hence the impacts of global warming. Minerals such as TiO₂ or SiO₂ are among the potentially suitable aerosol materials for stratospheric particle injection due to their greater light-scattering ability than stratospheric sulfuric acid particles. However, the heterogeneous reactivity of mineral particles towards trace gases important for stratospheric chemistry largely remains unknown, precluding reliable assessment of their impacts on stratospheric ozone, which is of key environmental significance. In this work we have investigated for the first time the heterogeneous hydrolysis of ClONO₂ on TiO₂ and SiO₂ aerosol particles at room temperature and at different relative humidities (RHs), using an aerosol flow tube. The uptake coefficient, γ (ClONO₂), on TiO₂ was $\sim 1.2 \times 10^{-3}$ at 7% RH and remained unchanged at 33% RH, and increased for SiO₂ from $\sim 2 \times 10^{-4}$ at 7% RH to $\sim 5 \times 10^{-4}$ at 35% RH, reaching a value of $\sim 6 \times 10^{-4}$ at 59% RH. We have also examined the impacts of a hypothetical TiO₂ injection on stratospheric chemistry using the UKCA (United Kingdom Chemistry and

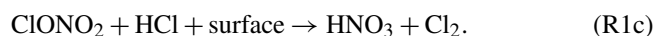
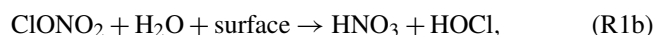
Aerosol) chemistry–climate model, in which heterogeneous hydrolysis of N₂O₅ and ClONO₂ on TiO₂ particles is considered. A TiO₂ injection scenario with a solar-radiation scattering effect very similar to the eruption of Mt Pinatubo was constructed. It is found that, compared to the eruption of Mt Pinatubo, TiO₂ injection causes less ClO_x activation and less ozone destruction in the lowermost stratosphere, while reduced depletion of N₂O₅ and NO_x in the middle stratosphere results in decreased ozone levels. Overall, no significant difference in the vertically integrated ozone abundances is found between TiO₂ injection and the eruption of Mt Pinatubo. Future work required to further assess the impacts of TiO₂ injection on stratospheric chemistry is also discussed.

1 Introduction

Climate engineering (also known as geoengineering), the deliberate and large-scale intervention in the Earth's climatic system to reduce global warming (Shepherd, 2009), has been actively discussed by research communities and is also beginning to surface in the public consciousness. The injection

of aerosol particles (or their precursors) into the stratosphere to scatter solar radiation back into space is one of the solar-radiation management (SRM) schemes proposed for climate engineering (Crutzen, 2006). Sulfuric acid particles, due to their natural presence in the stratosphere (SPARC, 2006), have been the main focus of stratospheric particle injection research (Crutzen, 2006; Ferraro et al., 2011; Kravitz et al., 2013; Tilmes et al., 2015; Jones et al., 2016). Very recently, minerals with refractive indices higher than sulfuric acid, e.g. TiO₂ and SiO₂, have been proposed as possible alternative particles to be injected into the stratosphere for climate engineering (Pope et al., 2012). For example, the refractive index at 550 nm is 2.5 for TiO₂ and 1.5 for stratospheric sulfuric acid particles. If the size of TiO₂ particles used for SRM can be optimised, it is estimated that compared to sulfuric acid particles, the use of TiO₂ requires a factor of ~ 3 less in mass (and a factor of ~ 7 less in volume) in order to achieve the same solar-radiation scattering effect (Pope et al., 2012).

Injecting particles into the stratosphere would increase the amount of aerosol particles in the stratosphere, thus increasing the surface area available for heterogeneous reactions (e.g. Reactions R1a, R1b and R1c), whose effects on stratospheric chemistry and in particular on stratospheric ozone depletion have been well documented for sulfuric acid particles (Molina et al., 1996; Solomon, 1999). The background burden of sulfuric acid particles in the stratosphere, i.e. during periods with low volcanic activities, is 0.65 ± 0.2 Tg (SPARC, 2006). The eruption of Mt Pinatubo in 1991 delivered an additional ~ 30 Tg sulfuric acid particles into the stratosphere (Guo et al., 2004) and subsequently produced record low levels of stratospheric ozone (McCormick et al., 1995), in addition to causing substantial surface cooling (Dutton and Christy, 1992). Observation and modelling studies have further suggested that, after the eruption of Mt Pinatubo, significant change in the partitioning of nitrogen and chlorine species in the stratosphere occurred (Fahey et al., 1993; Wilson et al., 1993; Solomon, 1999), caused by heterogeneous reactions of N₂O₅ and ClONO₂ (Reactions R1a–R1c):



Therefore, before any types of material can be considered for stratospheric particle injection, their impact on stratospheric chemistry and ozone in particular has to be well understood (Tilmes et al., 2008; Pope et al., 2012).

Heterogeneous reactions on sulfuric acid and polar stratospheric clouds (PSCs) have been extensively studied and well characterised (Crowley et al., 2010; Ammann et al., 2013; Burkholder et al., 2015). However, the reactivity of minerals (e.g. TiO₂ and SiO₂) towards reactive trace gases in the

stratosphere has received much less attention. For example, the heterogeneous reactions of ClONO₂ with silica (SiO₂) and alumina (Al₂O₃) in the presence of HCl (Reaction R1c) have only been explored by one previous study (Molina et al., 1997), in which minerals coated on the inner wall of a flow tube were used. Further discussion of this work is provided in Sect. 4.4. The lack of high-quality kinetic data for important reactions impedes reliable assessment of the impact of injecting mineral particles into the stratosphere on stratospheric ozone (Pope et al., 2012). TiO₂ is an active photocatalyst (Shang et al., 2010; Chen et al., 2012; Romanias et al., 2012; Kebede et al., 2013; George et al., 2015), and the effects of its photochemical reactions on stratospheric chemistry, if injected into stratosphere for the purpose of climate engineering, have never been assessed. Therefore, its atmospheric heterogeneous photochemistry deserves further investigation.

To address these issues, in our previous work we have investigated the heterogeneous reactions of N₂O₅ with TiO₂ (Tang et al., 2014c) and SiO₂ (Tang et al., 2014a) particles (Reaction R1a). That work is extended here to the investigation of the heterogeneous hydrolysis of ClONO₂ on TiO₂ and SiO₂ (Reaction R1b) using an aerosol flow tube. There are only a few previous studies in which the reactions of ClONO₂ with airborne particles or droplets have been examined. For example, the interaction of ClONO₂ with sulfuric acid aerosol particles has been investigated using aerosol flow tubes (Hanson and Lovejoy, 1995; Ball et al., 1998; Hanson, 1998). Droplet train techniques have been used to study the heterogeneous reactions of ClONO₂ with aqueous droplets containing sulfuric acid (Robinson et al., 1997) or halide (Deiber et al., 2004). The interaction of ClONO₂ with airborne water ice particles has also been examined (Lee et al., 1999). Our experimental work, carried out at room temperature and at different relative humidities (RHs), is the first study which has investigated the heterogeneous interaction of ClONO₂ with airborne mineral particles. In the lower stratosphere into which particles would be injected, typical temperature and RH ranges are 200–220 K and $< 40\%$, respectively (Dee et al., 2011). We note that, while our experimental work covers the RH range relevant for the lower stratosphere, it has only been performed at room temperature instead of 200–220 K due to experimental challenges.

ClONO₂ may also play a role in tropospheric chemistry (Finlayson-Pitts et al., 1989), though its presence in the troposphere has not yet been confirmed by field measurements. The importance of Cl atoms in tropospheric oxidation capacity has received increasing attention in recent years (Simpson et al., 2015), and precursors of Cl atoms – e.g. ClNO₂ (Osthoff et al., 2008; Thornton et al., 2010; Phillips et al., 2012; Bannan et al., 2015; Wang et al., 2016), Cl₂ (Spicer et al., 1998; Riedel et al., 2012; Liao et al., 2014) and HOCl (Lawler et al., 2011) – have been detected in the troposphere at various locations. Cl atoms react with O₃ to form ClO radicals, which react with NO₂ to produce ClONO₂. The uptake

of ClONO₂ by aerosol particles (Reactions R1b, R1c) may recycle ClONO₂ to more photolabile species (HOCl or Cl₂) and thus amplify the impact of Cl atoms on tropospheric oxidation capacity (Finlayson-Pitts et al., 1989; Deiber et al., 2004). Considering the widespread occurrence of reactive chlorine species (Simpson et al., 2015) and mineral dust particles (Textor et al., 2006; Ginoux et al., 2012; Tang et al., 2016) in the troposphere, our laboratory measurements can also have strong implications for tropospheric chemistry.

Using the UKCA (United Kingdom Chemistry and Aerosol) chemistry–climate model, a preliminary assessment of the effect of injecting TiO₂ into the stratosphere on stratospheric chemistry and ozone was discussed in our previous work (Tang et al., 2014c). This model has also been used to investigate stratospheric ozone change due to volcanic sulfuric acid particles after the eruption of Mt Pinatubo in 1991 (Telford et al., 2009). In the previous work (Tang et al., 2014c), we used the UKCA model to construct a case study in which TiO₂ aerosols were distributed in the stratosphere in a similar way to the volcanic sulfuric acid particles after the eruption of Mt Pinatubo so that the solar-radiation scattering effect was similar for the two scenarios; however, the only heterogeneous reaction on TiO₂ particles considered was the uptake of N₂O₅ (Reaction R1a). Injection of solid aerosols into the stratosphere can have a significant impact on ozone mixing ratios when heterogeneous reactions involving chlorine are considered (Weisenstein et al., 2015). Several previous studies (Jackman et al., 1998; Danilin et al., 2001; Weisenstein et al., 2015) have considered the effects of solid alumina particles on stratospheric chemistry; however, there is only very limited assessment of other potential solid aerosol compositions (e.g. TiO₂ and diamond) (Tang et al., 2014c). Here we expand upon the previous literature by considering in our model a number of heterogeneous reactions with new kinetic data on TiO₂. In our current work the heterogeneous hydrolysis of ClONO₂ on TiO₂ particles (Reaction R1b) has been included, using our new experimental data. The changes in stratospheric ozone and reactive nitrogen and chlorine species are assessed by comparing to the impact of the Mt Pinatubo eruption.

2 Experimental section

The heterogeneous reaction of ClONO₂ with aerosol particles was investigated at different RHs using an atmospheric pressure aerosol flow tube (AFT). In addition, its uptake onto Pyrex glass was also studied, using a coated-wall flow tube. N₂ was used as a carrier gas, and all the experiments were carried out at 296 ± 2 K.

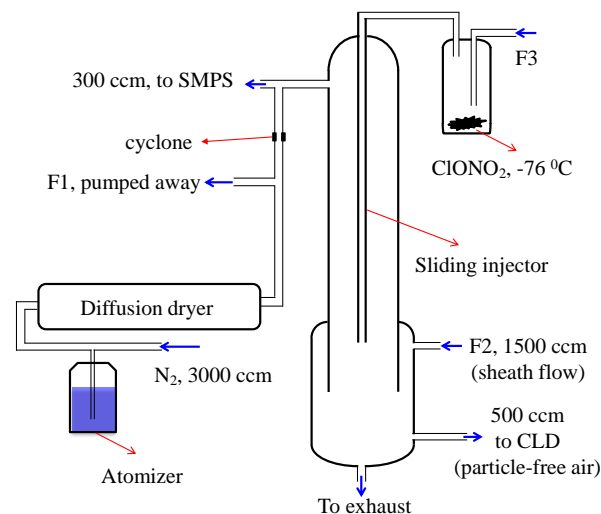


Figure 1. Schematic diagram of the aerosol flow tube used in this study. SMPS: scanning mobility particle sizer; CLD: chemiluminescence detector, used to measure the ClONO₂ concentration (measured as the change in NO concentration). All the flows (except the flow applied to the atomiser) were controlled by mass flow controllers. Flow details are provided in the text.

2.1 Aerosol flow tube

2.1.1 Flow tube

A detailed description of the AFT was given in our previous work (Tang et al., 2014a, c), and only the key features are described here. The flow tube, as shown in Fig. 1, is a horizontally mounted Pyrex glass tube (ID: 3.0 cm; length: 100 cm). The total flow in the AFT was 1500 mL min⁻¹, leading to a linear flow velocity of 3.54 cm s⁻¹ and a maximum residence time of ~ 30 s. The Reynolds number is calculated to be 69, suggesting a laminar flow condition in the flow tube. Under our experimental conditions, the entrance length needed to develop the laminar flow is ~ 12 cm. The mixing length is calculated to be ~ 14 cm, using a diffusion coefficient of 0.12 cm² s⁻¹ for ClONO₂ in N₂ at 296 K (Tang et al., 2014b). Only the middle part of the flow tube (30–80 cm) was used to measure the uptake kinetics.

A commercial atomiser (Model 3076, TSI, USA) was used to generate an ensemble of mineral aerosols. N₂ at ~ 3 bar was applied to the atomiser to disperse the mineral–water mixture (with a TiO₂ or SiO₂ mass fraction of ~ 0.5 %), resulting in an aerosol flow of 3000 mL min⁻¹. The aerosol flow was delivered through two diffusion dryers, and the resulting RH was adjusted by varying the amount of silica gel in the diffusion dryers. A flow of 1200 mL min⁻¹ was pumped away through F1, and the remaining flow (1800 mL min⁻¹) was then delivered through a cyclone (TSI, USA) to remove super-micrometre particles. This cyclone has a cut-off size of 800 nm at a flow rate of 1000 mL min⁻¹. The aerosol flow could be delivered through a filter to re-

move all the particles (to measure the wall loss rate), or alternatively the filter could be bypassed to introduce aerosol particles into the AFT (to measure the total loss rate). Beyond that point, 300 mL min⁻¹ was sampled by a scanning mobility particle sizer (SMPS), and the remaining 1500 mL min⁻¹ flow was delivered into the AFT via the side arm. Mineral aerosols were characterised online using a SMPS, consisting of a differential mobility analyser (DMA, TSI 3081) and a condensation particle counter (CPC, TSI 3775) which was operated with a sampling flow rate of 300 mL min⁻¹. The sheath flow of the DMA was set to 2000 mL min⁻¹, giving a detectable mobility size range of 19–882 nm. The time resolution of the SMPS measurement was 150 s.

The bottom 30 cm of the AFT was coaxially inserted into another Pyrex tube (inner diameter: 4.3 cm; length: 60 cm). A sheath flow (F2, 1500 mL min⁻¹) was delivered through the annular space between the two coaxial tubes. The sheath flow has the same linear velocity as the aerosol flow to minimise the turbulence at the end of the aerosol flow tube where the two flows joined. Gases could exchange between the sheath flow and the aerosol flow because of their large diffusion coefficients ($\sim 0.1 \text{ cm}^2 \text{ s}^{-1}$) (Tang et al., 2014b), while aerosol particles remained in the centre due to their much smaller diffusion coefficients, i.e. 10^{-7} – $10^{-6} \text{ cm}^2 \text{ s}^{-1}$ (Hinds, 1996). At the end of the large Pyrex tube, a flow of 500 mL min⁻¹ was sampled through a 1/4 in. fluorinated ethylene propylene (FEP) tube which intruded 1–2 mm into the flow close to the wall of the Pyrex tube. This gas–particle separation method enabled particle-free gas to be sampled, despite very high aerosol concentrations used in the AFT. Sampling particle-free gas prevents particles from deposition onto the inner wall of the sampling tube and therefore minimises the undesired loss of the reactive trace gases (e.g. ClONO₂ in this study) during their transport to the detector. More detailed discussion of this gas–particle separation method used in the aerosol flow experiments is provided elsewhere (Rouviere et al., 2010; Tang et al., 2012).

2.1.2 ClONO₂ synthesis

ClONO₂ was synthesised in the lab by reacting Cl₂O with N₂O₅ (Davidson et al., 1987; Fernandez et al., 2005). N₂O₅ crystals were synthesised by trapping the product formed from mixing NO with O₃ in large excess (Fahey et al., 1985). The synthesis and purification are detailed in our previous study (Tang et al., 2014c). Cl₂O was synthesised by reacting HgO with Cl₂ (Renard and Bolker, 1976; Molina et al., 1977). Cl₂ from a lecture bottle was first trapped as yellow-green liquid (a few millilitres) in a glass vial at -76°C using an ethanol–dry-ice bath. It was then warmed up to room temperature so that all the Cl₂ was evaporated and transferred to the second glass vessel, which contained HgO powders in excess and was kept at -76°C . The glass vessel containing liquid Cl₂ and HgO powders was sealed and kept at -76°C overnight. It was then warmed up to room temperature to

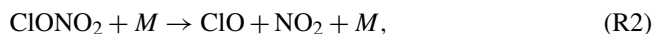
evaporate and transfer the formed Cl₂O and any remaining Cl₂ to the third glass vial kept at -76°C . Liquid Cl₂O appeared dark reddish-brown in colour.

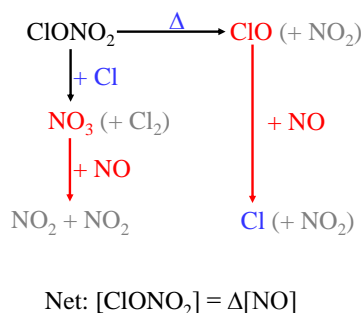
The third vessel containing Cl₂O was warmed up to room temperature to evaporate and transfer Cl₂O to the fourth vial, which contained synthesised N₂O₅ and was kept at -76°C . The vial containing Cl₂O and N₂O₅ was sealed and kept at -50°C for 2–3 days in a cryostat. In this work Cl₂O was in slight excess compared to N₂O₅, and thus all the white powder (solid N₂O₅) was consumed. ClONO₂ is liquid at -50°C , with a colour similar to liquid Cl₂. The major impurity of our synthesised ClONO₂ was Cl₂O, and the boiling temperature at 760 torr is 2 °C for Cl₂O and $\sim 22^\circ\text{C}$ for ClONO₂ (Stull, 1947; Renard and Bolker, 1976). To purify our synthesised ClONO₂, the vial containing ClONO₂ was warmed up to 5 °C and connected to a small dry-N₂ flow via a T-piece for a few hours. Note that the N₂ flow was not delivered into the vial but instead served as a dry atmosphere at ~ 760 torr. Cl₂O was boiled at 5 °C and diffused passively into the N₂ flow. Cl₂ was also removed because its boiling temperature is -34°C (Stull, 1947). The amount of N₂O₅ in ClONO₂ was minimised because Cl₂O was in excess. In addition, the vapour pressure (a few millitorr) of N₂O₅ (Stull, 1947) is > 100 times lower than that of ClONO₂ (~ 1 torr) at around -76°C (Schack and Lindahl, 1967; Ballard et al., 1988; Anderson and Fahey, 1990); therefore, even if N₂O₅ were present in the gas phase, its amount would be negligible compared to ClONO₂.

2.1.3 ClONO₂ detection

The ClONO₂ vial was stored at -76°C in the dark using a cryostat. A small dry-N₂ flow (a few millilitres per minute, F3) was delivered into the vial to elute gaseous ClONO₂. The ClONO₂ flow was delivered through 1/8 in. FEP tubing in a stainless-steel injector into the centre of the aerosol flow tube. The position of the injector could be adjusted to vary the interaction time of ClONO₂ with aerosols in the flow tube.

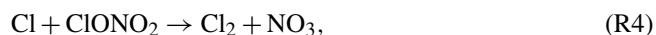
The flow sampled from the flow tube (500 mL min⁻¹) was mixed with $\sim 5 \text{ mL min}^{-1}$ NO (100 ppmv in N₂) and then delivered into a glass reactor heated to 130 °C. The initial NO mixing ratio (in the absence of ClONO₂) in the reactor was ~ 1000 ppbv (or $\sim 1.8 \times 10^{13} \text{ molecule cm}^{-3}$). The volume of the glass reactor (inner diameter: 2.0 cm; length: 10 cm) is $\sim 30 \text{ cm}^3$, corresponding to an average residence time of ~ 2.6 s at 130 °C. The scheme used in our work to detect ClONO₂ is shown in scheme 1 and explained in detail below. ClONO₂ was thermally decomposed in the reactor to ClO and NO₂ (Reaction R2, where *M* is the third molecule, e.g. N₂), and ClO was then titrated by NO in excess (Reaction R3):





Scheme 1. The ClONO₂ detection scheme used in our work.

Cl atoms produced in Reaction (R3) further reacted with ClONO₂ (Reaction R4), and the NO₃ radicals formed were titrated by NO (Reaction R5):



If the thermal dissociation of ClONO₂ (Reaction R2) and the scavenging of ClO and NO₃ radicals by NO (Reactions R3, R4) all reach completion, the initial mixing ratio of ClONO₂ is equal to the decrease in the NO mixing ratios before and after introducing ClONO₂ into the reactor (Anderson and Fahey, 1990).

The lifetime of ClONO₂ with respect to thermal dissociation (Reaction R2) at 130 °C was estimated to be ~0.2 s at 160 torr (Anderson and Fahey, 1990), and further increase in pressure to ~760 torr would increase the decomposition rate and reduce its lifetime. The lifetime of ClONO₂ with respect to Reaction (R4) is not critical for our purpose, although it enhances the overall decay of ClONO₂ in the reactor. The second-order rate constants are $1.3 \times 10^{-11} \text{ cm}^3 \text{ molecule}^{-1} \text{ s}^{-1}$ for the reaction of ClO with NO and $2.3 \times 10^{-11} \text{ cm}^3 \text{ molecule}^{-1} \text{ s}^{-1}$ for the reaction of NO₃ with NO at 130 °C (Burkholder et al., 2015), giving lifetimes of ~4 × 10⁻³ s for ClO with respect to Reaction (R3) and ~2 × 10⁻³ s for NO₃ with respect to Reaction (R5) in the presence of ~1000 ppbv NO in the reactor. To conclude, under our experimental conditions, the residence time of the gas flow in the heated reactor was long enough for the completion of thermal dissociation of ClONO₂ (Reaction R2) and titrations of ClO and NO₃ by NO (Reactions R3 and R5).

The flow exiting the reactor was sampled by a chemiluminescence-based NO_x analyser (Model 200E, Teledyne Instruments, USA), which has a sampling flow rate of 500 mL min⁻¹ (±10%). This instrument has two modes. In the first mode NO is measured by detecting the chemiluminescence of exited NO₂ (NO₂^{*}) produced by reacting NO with O₃ in excess. The gas flow can also be passed through a convertor cartridge filled with molybdenum (Mo) chips heated to 315 °C, and all the NO₂ (and very likely also some of other NO_y, e.g. HONO, HNO₃) is converted to NO; in this mode the total NO (initial NO, NO converted from NO₂

etc.) is measured and termed NO_x. The two modes are periodically switched, and the instrument has a detection limit of 0.5 ppbv with a time resolution of 1 min.

The response of measured NO and NO_x mixing ratios to the introduction of ClONO₂ into the AFT is displayed in Fig. 2. Both the sheath flow and the flow in the AFT were set to 1500 mL min⁻¹ (dry N₂), and the injector was at 40 cm. The introduction of ClONO₂ into the AFT at ~20 min leads to the decrease of NO (solid curve in Fig. 2a) from ~1100 to ~400 ppbv, and NO recovered to its initial level after stopping the ClONO₂ flow at ~120 min. The ClONO₂ mixing ratio (solid curve in Fig. 2b), derived from the change in the NO mixing ratio, was very stable over 100 min. As expected, the introduction of ClONO₂ into the system led to the increase of the measured NO_x mixing ratio (dashed curve in Fig. 2a). Ideally the increase in NO_x mixing ratios due to the introduction of ClONO₂ should be equal to the ClONO₂ mixing ratio. The nitrogen balance (dashed curve in Fig. 2b), defined as the difference in the ClONO₂ mixing ratios (equal to the change in NO mixing ratios) and the change of the NO_x mixing ratios, is essentially zero within the experimental noise level. This gives us further confidence in the purity of our synthesised ClONO₂: under our current detection scheme the change in the NO_x mixing ratios will be twice that of the N₂O₅ mixing ratio, and therefore N₂O₅ contained in the ClONO₂ flow as an impurity was negligible. This method provides a simple and relatively selective method to quantify ClONO₂, and it could be used to calibrate other ClONO₂ detection methods (Anderson and Fahey, 1990). One previous study used a similar method to detect ClONO₂ in its experiments of ClONO₂ uptake onto sulfuric acid aerosol particles (Ball et al., 1998), with the only difference being that in that study NO was detected by its absorption at 1845.5135 cm⁻¹. Their reported $\gamma(\text{ClONO}_2)$ onto sulfuric acid aerosol particles are in good agreement with those measured by other studies in which ClONO₂ was measured using mass spectrometry. This suggests that the indirect detection method of ClONO₂ utilised by Ball et al. (1998) and in this work can be used to investigate the uptake of ClONO₂ onto aerosol particles.

2.2 Coated-wall flow tube

The coated-wall flow tube, a Pyrex glass tube with an inner diameter of 30 mm, was used to measure the uptake of ClONO₂ onto fresh Pyrex glass. The inner wall was rinsed with diluted NaOH solution and then by methanol and deionised water. A flow of 1500 mL min⁻¹, humidified to the desired RH, was delivered into the top of the flow tube via a side arm. A small N₂ flow was used to elute the liquid ClONO₂ sample, and the flow was then delivered through a 1/8 in. Teflon tube in a stainless-steel injector into the centre of the flow tube. The position of the injector could be changed to vary the interaction time between ClONO₂ and the inner wall of the flow tube. At the bottom of the flow

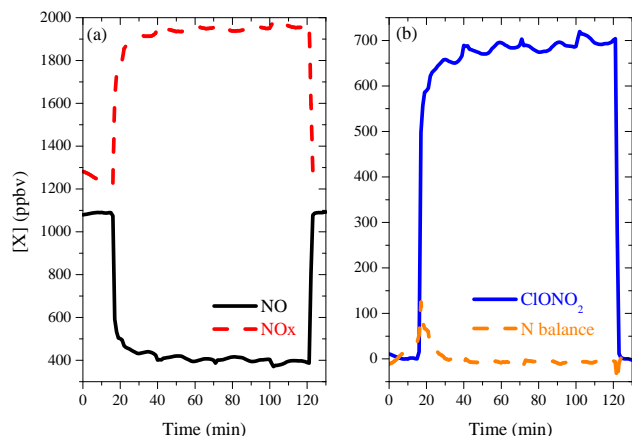


Figure 2. Response of measured NO and NO_x mixing ratios to the introduction of ClONO₂ into the flow tube (left panel). The corresponding calculated ClONO₂ mixing ratio and nitrogen balance are also shown (right panel).

tube, a flow of 500 mL min⁻¹ was sampled through another side arm, mixed with ~5 mL min⁻¹ NO (100 ppmv in N₂) and then delivered into a glass reactor heated to 130 °C. The flow exiting the heated glass reactor was then sampled into a NO_x analyser. The method used to detect ClONO₂ is detailed in Sect. 2.1. The remaining flow (~1000 mL min⁻¹) went through a RH sensor into the exhaust.

The linear flow velocity in the flow tube is 3.54 cm s⁻¹ with a Reynolds number of 69, suggesting that the flow is laminar. The length of the flow tube, defined as the distance between the side arm through which the main flow was delivered into the flow tube and the other side arm through which 500 mL min⁻¹ was sampled from the flow tube into the NO_x analyser, is 100 cm, giving a maximum residence time of ~30 s. The entrance length required to fully develop the laminar flow and the mixing length required to fully mix ClONO₂ with the main flow are both less than 15 cm. The loss of ClONO₂ onto the inner wall was measured using the middle part (30–80 cm) of the flow tube.

2.3 Chemicals

NO (>99% purity) in a lecture bottle and the 100 ppmv (±1 ppmv) of NO in N₂ were supplied by CK Special Gas (UK). Pure Cl₂ (with a purity of >99.5%) in a lecture bottle and HgO (yellow powder, with a purity of >99%) were provided by Sigma-Aldrich (UK). N₂ and O₂ were provided by BOC Industrial Gases (UK). P25 TiO₂, with an anatase-to-rutile ratio of 3:1, was supplied by Degussa-Hüls AG (Germany). SiO₂ powders with a stated average particle size (aggregate) of 200–300 nm were purchased from Sigma-Aldrich (UK). The Brunauer–Emmett–Teller (BET) surface area is 8.3 m² g⁻¹ for TiO₂ (Tang et al., 2014c) and ~201 m² g⁻¹ for SiO₂ (Tang et al., 2014a).

3 Model description

The UKCA chemistry–climate model in its coupled stratosphere–troposphere configuration, which combines both the tropospheric (O’Connor et al., 2014) and stratospheric (Morgenstern et al., 2009) schemes, was used to simulate the effect of heterogeneous hydrolysis of N₂O₅ (Reaction R1a) and ClONO₂ (Reaction R1b) on TiO₂. In this model the chemical cycles of O_x, HO_x and NO_x; the oxidation of CO, ethane, propane and isoprene; and chlorine and bromine chemistry are all included. The model also includes a detailed treatment of polar processes. UKCA uses an equilibrium scheme to determine the presence and abundance of nitric acid trihydrate (NAT) and ice PSCs, assuming thermodynamic equilibrium with gas-phase HNO₃ and water vapour (Chipperfield, 1999). Chlorine activation through heterogeneous reactions occurs on both PSC particles and sulfuric acid aerosols (Morgenstern et al., 2009).

The same approach used to investigate the effects of the eruption of Mt Pinatubo on stratospheric ozone (Telford et al., 2009) is adopted in this study. Using the UKCA model in a “nudged” configuration, Telford et al. (2009) evaluated the difference of stratospheric ozone with and without the additional sulfuric acid aerosols caused by the eruption of Mt Pinatubo. “Nudging”, or Newtonian relaxation, is a method that provides a realistic representation of short-term dynamical features by adjusting modelled dynamical variables towards meteorological reanalysis data. This process was detailed by a previous study (Telford et al., 2008) and has been used in a number of other models (Jeuken et al., 1996; Takemura et al., 2000; Hauglustaine et al., 2004; Schmidt et al., 2006). By constraining the dynamics of the model in this way, the model is able to faithfully reproduce the meteorology of the time period around the eruption of Mt Pinatubo.

In our current study three simulations are used to assess the effects of TiO₂ particle injection into the stratosphere. All three simulations are started from a spun-up initial condition and run from December 1990 to January 1993. In the base scenario (S1), an aerosol climatology is used which represents the background loading of stratospheric sulfate aerosol. Alongside S1 two further simulations were performed, one representing the eruption of Mt Pinatubo in June 1991 (S2) and a second (S3) in which the Mt Pinatubo eruption is replaced with a single injection of TiO₂ particles on the same date. The simulations are set up so that the radiative impacts at the surface are comparable between S2 and S3. Pope et al. (2012) have proposed that 10 Tg of TiO₂ aerosol particles with an assumed radius of 70 nm are required in order to achieve the same solar-radiation scattering effect as the eruption of Mt Pinatubo. The total surface area of TiO₂ is calculated from the mass of TiO₂ particles, using a density of 4.23 g cm⁻³ and an assumed radius of 70 nm, and the global distribution of TiO₂ is scaled to the sulfuric acid aerosol distribution resulting from the eruption of Mt Pinatubo. The sulfuric acid aerosol surface area distribution was derived

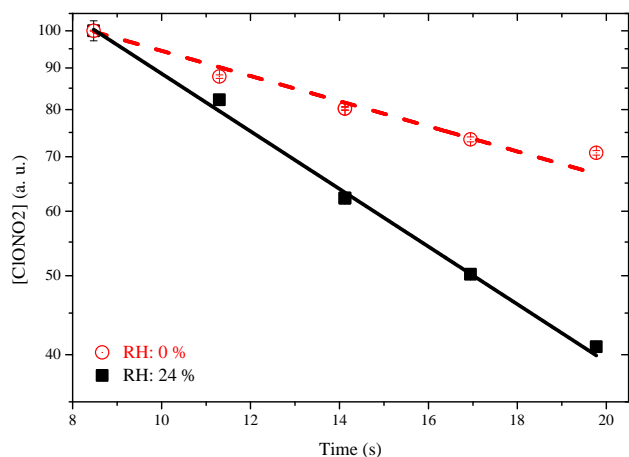


Figure 3. Decays of ClONO₂ in the flow tube due to its loss onto the Pyrex glass (circles: 0 % RH; squares: 24 % RH). Measured ClONO₂ mixing ratios were normalised to that at 8.5 s (when the injector was at 30 cm). Typical ClONO₂ mixing ratios in the flow tube are a few hundred parts per billion by volume (ppbv; see Fig. 2).

from the Stratosphere–troposphere Processes And their Role in Climate (SPARC) climatology (SPARC, 2006).

By running these three scenarios, we are able to compare the relative impact of stratospheric particle injection using TiO₂ compared to sulfate. The benefit of using the Mt Pinatubo eruption as the sulfate injection scenario is that it provides a natural analogue to proposed climate engineering schemes, and the chemical and dynamical effects of the eruption have been well documented. Telford et al. (2009) have shown that UKCA accurately models the chemical impacts of the Mt Pinatubo eruption, and the ozone bias is smaller now than in Telford et al. (2009).

It should be noted that all simulations are nudged to the same observed meteorological conditions, following Telford et al. (2008). In this way we do not take into account the radiative/dynamical feedbacks from any ozone changes resulting from chemical reactions occurring on stratospheric aerosols, allowing just the chemical effects of stratospheric particle injection to be quantified. The results presented here expand on our previous study (Tang et al., 2014c) by including heterogeneous hydrolysis of both N₂O₅ (Reaction R1a) and ClONO₂ (Reaction R1b) on TiO₂. An uptake coefficient of 1.5×10^{-3} is used for Reaction R1a (reaction with N₂O₅) on TiO₂ particles as determined by our previous measurement (Tang et al., 2014c). An uptake coefficient of 1.5×10^{-3} is used for Reaction R1b (heterogeneous hydrolysis of ClONO₂). Considering errors in measurements, this value agrees with experimental $\gamma(\text{ClONO}_2)$, which was determined to be $\sim 1.2 \times 10^{-3}$ in our work as shown in Table 2.

Table 1. Loss rates (k_w), effective uptake coefficients (γ_{eff}) and true uptake coefficients (γ) of ClONO₂ onto the inner wall of the Pyrex tube at different relative humidities (RHs). Measurements were all carried out with initial ClONO₂ mixing ratios of several hundred ppbv.

RH (%)	$k_w (\times 10^{-2} \text{ s}^{-1})$	$\gamma_{\text{eff}} (\times 10^{-6})$	$\gamma (\times 10^{-6})$
0	3.6 ± 0.2	4.2 ± 0.3	5.1 ± 0.3
	2.9 ± 0.4	3.4 ± 0.5	3.9 ± 0.6
6	4.1 ± 0.1	4.9 ± 0.1	6.2 ± 0.1
	3.7 ± 0.7	4.4 ± 0.8	5.4 ± 1.0
12	4.1 ± 0.3	4.9 ± 0.4	6.2 ± 0.5
17	6.9 ± 0.3	8.2 ± 0.4	13 ± 0.6
	6.4 ± 0.2	7.6 ± 0.2	11 ± 0.4
24	8.1 ± 0.8	9.6 ± 1.0	16 ± 2.0
	8.2 ± 0.3	9.6 ± 0.4	17 ± 0.7

4 Results and discussion

4.1 Uptake of ClONO₂ onto Pyrex glass

The uptake of ClONO₂ onto a fresh Pyrex glass wall was determined by measuring the ClONO₂ concentrations at five different injection positions. The loss of ClONO₂ in the coated-wall flow tube, under the assumption of pseudo-first-order kinetics, can be described by Eq. (1):

$$[\text{ClONO}_2]_t = [\text{ClONO}_2]_0 \cdot \exp(-k_w \cdot t), \quad (1)$$

where $[\text{ClONO}_2]_t$ and $[\text{ClONO}_2]_0$ are the measured ClONO₂ concentrations at the reaction time of t and 0, respectively, and k_w is the wall loss rate (s^{-1}). Two typical datasets of measured $[\text{ClONO}_2]$ at five different injector positions are displayed in Fig. 3, suggesting that ClONO₂ indeed follows the exponential decays, and the slopes of the exponential decays are equal to k_w . The effective (or experimental) uptake coefficient of ClONO₂, γ_{eff} , onto the Pyrex wall can then be calculated from k_w , using Eq. (2) (Howard, 1979; Wagner et al., 2008):

$$\gamma_{\text{eff}} = \frac{k_w \cdot d_{\text{tube}}}{c(\text{ClONO}_2)}, \quad (2)$$

where d_{tube} is the inner diameter of the flow tube (3.0 cm) and $c(\text{ClONO}_2)$ is the average molecular speed of ClONO₂ ($25\,360 \text{ cm s}^{-1}$). Depletion of ClONO₂ close to the wall is caused by the uptake of ClONO₂ onto the wall, and thus the effective uptake coefficient is smaller than the true one. This effect can be corrected (Tang et al., 2014b), and true uptake coefficients, γ , are reported in Table 1 together with the corresponding wall loss rates (k_w) and effective uptake coefficients (γ_{eff}).

The uptake coefficients of ClONO₂ onto Pyrex glass, as summarised in Table 1, increases from $\sim 5 \times 10^{-6}$ at 0 % RH to $\sim 1.6 \times 10^{-5}$ at 24 % RH by a factor of ~ 3 . Uptake coefficients at higher RH were not determined because the uptake

coefficients determined at 24 % RH ($\sim 1.6 \times 10^{-5}$) are very close to the upper limit ($\sim 2.3 \times 10^{-5}$), which can be measured in this study using the coated-wall flow tube technique due to the gas-phase diffusion limit. The RH dependence of $\gamma(\text{ClONO}_2)$ for Pyrex glass is further discussed in Sect. 4.4 together with those reported by Molina et al. (1997) and our measurements on SiO₂ and TiO₂ aerosol particles.

4.2 Reaction of ClONO₂ with SiO₂ and TiO₂ particles

The uptake of ClONO₂ onto airborne SiO₂ and TiO₂ particles was investigated using an atmospheric pressure aerosol flow tube, in which reactions with the aerosol particles and the wall both contribute to the loss of ClONO₂, as shown in Eq. (3):

$$[\text{ClONO}_2]_t = [\text{ClONO}_2]_0 \cdot \exp[-(k_w + k_a) \cdot t], \quad (3)$$

where $[\text{ClONO}_2]_t$ and $[\text{ClONO}_2]_0$ are the measured ClONO₂ mixing ratios at the reaction times of t and 0 s, and k_w and k_a are the loss rates (s^{-1}) of ClONO₂ onto the inner wall of the flow tube and the surface of aerosol particles, respectively. In a typical uptake measurement, the aerosol flow was delivered through a filter, and $[\text{ClONO}_2]$ was measured at five different injector positions to determine the wall loss rate (k_w). The filter was then bypassed to deliver aerosol particles into the flow tube, and the total ClONO₂ loss rate ($k_w + k_a$) in the flow tube was determined. After that, the aerosol flow was passed through the filter to measure k_w again. The variation of k_w determined before and after introducing particles into the flow tube was within the experimental uncertainty of k_w , ensuring that the reactivity of the wall towards ClONO₂ remained constant during the uptake measurement. Axial and radical diffusion of ClONO₂ could lead to biases in its measured loss rates in a flow tube, and this effect, though very small ($< 10\%$ in our work), has been corrected (Brown, 1978).

The difference between the ClONO₂ loss rates without and with aerosol particles in the flow tube is equal to the loss rate due to the reaction with the surface of aerosol particles (k_a). The effective uptake coefficient of ClONO₂ onto aerosol particles, γ_{eff} , is related to k_a by Eq. (4) (Crowley et al., 2010):

$$k_a = 0.25 \cdot \gamma_{\text{eff}} \cdot c(\text{ClONO}_2) \cdot S_a, \quad (4)$$

where S_a is the aerosol surface area concentration which can be derived from size-resolved number concentrations (as shown in Fig. S1 in the Supplement) measured by the SMPS. Uptake of ClONO₂ onto aerosol particles also leads to the depletion of ClONO₂ near the particle surface, and so the effective uptake coefficient is smaller than the true uptake coefficient. This effect, which can be corrected using the method described elsewhere (Tang et al., 2014b), is only a few percent in this study as the particle diameters are $< 1 \mu\text{m}$ and the uptake coefficient is relatively small ($\sim 1 \times 10^{-3}$).

Two typical decays of ClONO₂ in the aerosol flow tube without and with SiO₂/TiO₂ aerosol particles in the flow

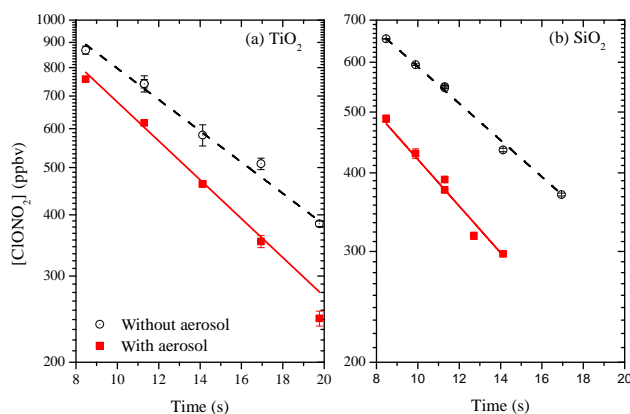


Figure 4. Decays of ClONO₂ in the aerosol flow tube without (open circles) and with (solid squares) aerosol particles in the aerosol flow tube under different experimental conditions. **(a)** TiO₂ with a surface area concentration of $2.3 \times 10^{-3} \text{ cm}^2 \text{ cm}^{-3}$ at 33 % RH; **(b)** SiO₂ with a surface area concentration of $2.9 \times 10^{-3} \text{ cm}^2 \text{ cm}^{-3}$ at 39 % RH.

tube are shown in Fig. 4. For a majority of experiments, efforts were made to generate enough aerosol particles so that $k_a + k_w$ was significantly different to k_w . It is evident from Fig. 4 that the loss of ClONO₂ is significantly faster with TiO₂/SiO₂ particles in the flow tube than without aerosols. We acknowledge that the measured k_a and therefore our reported γ in this study have quite large uncertainties. This is because the uptake coefficients of ClONO₂ are very small and the surface area of the wall is ~ 1000 times larger than that of aerosol particles. This is the first time that heterogeneous reactions of ClONO₂ with airborne mineral particles have been investigated.

The uptake coefficients of ClONO₂ are $\sim 1.2 \times 10^{-3}$ for TiO₂ particles, and no difference in $\gamma(\text{ClONO}_2)$ at two different RHs (7 and 33 %) is found. The heterogeneous reaction of ClONO₂ with SiO₂ particles was studied at four different RHs, with $\gamma(\text{ClONO}_2)$ increasing from $\sim 2 \times 10^{-4}$ at 7 % RH to $\sim 5 \times 10^{-4}$ at 35 % RH, reaching a value of $\sim 6 \times 10^{-4}$ at 59 % RH. The uptake coefficients of ClONO₂ are summarised in Table 2 for SiO₂ and TiO₂ aerosol particles, together with key experimental conditions. It should be pointed out that our measurements were carried out with ClONO₂ mixing ratios of several hundred parts per billion by volume (ppbv), significantly higher than those found in the lower stratosphere. Therefore, our measurements could underestimate $\gamma(\text{ClONO}_2)$ under stratospheric conditions. In a few measurements in which the SiO₂ aerosol concentrations were relatively low, the total ClONO₂ loss rate ($k_w + k_a$) was not different from its wall loss rate (k_w) within the experimental uncertainty. In this case, only the upper limit of k_a (and thus γ) can be estimated, which is reported here as the standard deviation of k_w . The first three of the four uptake coefficients at $(17 \pm 2)\%$ RH for SiO₂ aerosol particles, tabulated in Table 2, fall into this category. $\gamma(\text{ClONO}_2)$ on SiO₂

Table 2. Uptake coefficients of ClONO₂ onto SiO₂ and TiO₂ aerosol particles at different RHs. k_a : loss rate of ClONO₂ onto aerosol particle surface; S_a : aerosol surface area concentration; $\gamma(\text{ClONO}_2)$: uptake coefficients of ClONO₂. Measurements were all carried out with initial ClONO₂ mixing ratios of several hundred ppbv.

Particle	RH (%)	k_a ($\times 10^{-3}$ s)	S_a ($\times 10^{-3}$ cm ² cm ⁻³)	$\gamma(\text{ClONO}_2)$ ($\times 10^{-4}$)
SiO ₂	7 ± 1	4.1 ± 2.5	2.80 ± 0.02	2.3 ± 1.4
	7 ± 1	3.4 ± 3.2	2.78 ± 0.05	1.9 ± 1.8
	17 ± 2	< 5.1*	1.08 ± 0.08	< 7.5*
	17 ± 2	< 5.4*	1.28 ± 0.07	< 6.7*
	17 ± 2	< 7.3*	1.78 ± 0.09	< 6.5*
	17 ± 2	6.5 ± 4.2	2.08 ± 0.06	4.9 ± 3.2
	35 ± 4	6.3 ± 3.1	2.34 ± 0.08	4.2 ± 2.1
	35 ± 4	13.1 ± 4.7	2.91 ± 0.09	7.1 ± 2.6
	35 ± 4	9.0 ± 7.3	2.86 ± 0.10	4.8 ± 3.9
	59 ± 3	11.6 ± 3.5	2.88 ± 0.06	6.4 ± 1.9
TiO ₂	7 ± 1	7.0 ± 1.4	1.09 ± 0.12	10.1 ± 2.0
	7 ± 1	6.2 ± 2.3	0.73 ± 0.05	13.7 ± 5.0
	33 ± 3	17.9 ± 5.6	2.23 ± 0.03	12.7 ± 3.9
	33 ± 3	14.5 ± 1.4	1.93 ± 0.03	11.9 ± 1.1

* Estimated upper limits.

aerosol particles is around 2 orders of magnitude larger than that on Pyrex glass. One explanation for such a large difference is that SiO₂ particles used in our work are porous (Tang et al., 2014a), and therefore the surface area which is actually available for the ClONO₂ uptake is much larger than that calculated using the mobility diameters. In our previous study (Tang et al., 2014a) we have found that, for SiO₂ particles, $\gamma(\text{N}_2\text{O}_5)$ calculated using the mobility-diameter-based surface area are a factor of 40 larger than those calculated using the BET surface area. Another reason is that the composition of SiO₂ is different from Pyrex.

4.3 Effects of RH

The RH dependence of $\gamma(\text{ClONO}_2)$ for Pyrex glass is plotted in Fig. 5 and exhibits a positive dependence on RH, with $\gamma(\text{ClONO}_2)$ increased by a factor of ~ 3 when RH increases from 0 to 24%. Previous studies (Hanson and Ravishankara, 1991, 1994; Zhang et al., 1994; Hanson, 1998) have shown that $\gamma(\text{ClONO}_2)$ for aqueous H₂SO₄ solution strongly depends on water content in the solution, and it decreases from ~ 0.1 for 40% H₂SO₄ to $\sim 1 \times 10^{-4}$ for 75% H₂SO₄ at 200–200 K, by a factor of ~ 1000 . It is suggested that the heterogeneous uptake of ClONO₂ by aqueous H₂SO₄ solution proceeds via direct and acid-catalysed hydrolysis (Robinson et al., 1997; Shi et al., 2001; Ammann et al., 2013). One may expect that $\gamma(\text{ClONO}_2)$ for Pyrex glass will increase with RH. This is also supported by the water adsorption isotherm on Pyrex glass particles (Chikazawa et al., 1984), showing that the amount of adsorbed water on the Pyrex surface displays a substantial increase at 20% RH compared to that at 0% RH. However, the results reported by Chikazawa

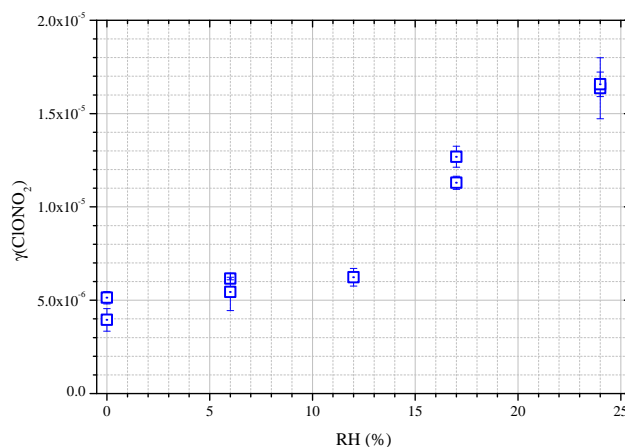


Figure 5. Dependence of $\gamma(\text{ClONO}_2)$ on RH for Pyrex glass.

et al. (1984) are presented graphically and thus impede us from a more quantitative discussion on the effect of RH and surface-adsorbed water on uptake of ClONO₂ by the Pyrex surface.

One can then expect that $\gamma(\text{ClONO}_2)$ may also increase with RH for the reaction with SiO₂ and TiO₂ aerosol particles, since the amount of water adsorbed on these two types of particles also increases with RH (Goodman et al., 2001). Inspection of the data listed in Table 2 reveals that $\gamma(\text{ClONO}_2)$ for SiO₂ particle increases from $\sim 2 \times 10^{-4}$ at 7% RH to $\sim 6 \times 10^{-4}$ at 59% RH, and this is consistent with the large increase of adsorbed water on the SiO₂ surface, from around half a monolayer at ~ 7 % RH to two monolayers at 60% RH (Goodman et al., 2001), as shown in Fig. S2.

The uptake coefficients of ClONO₂ were measured to be $\sim 1.2 \times 10^{-3}$ for TiO₂ at 7 and 33 % RH, with no significant difference found at these two different RHs. We expect that further increase in RH will lead to larger $\gamma(\text{ClONO}_2)$ for TiO₂, and future studies at higher RH are needed to better understand the RH effects.

At similar RH (7 and 33 %), $\gamma(\text{ClONO}_2)$ for TiO₂ are significantly larger than those for SiO₂. This may be explained by the larger amount of adsorbed water on TiO₂ at low and medium RH than on SiO₂ as shown in Fig. S2. It is interesting to note that the uptake of N₂O₅ shows different behaviour; i.e. $\gamma(\text{N}_2\text{O}_5)$ for SiO₂ (Tang et al., 2014a) are significantly larger than that for TiO₂ at similar RH. This may indicate that a different mechanism controls N₂O₅ uptake by mineral surfaces. However, mechanistic explanations of the different heterogeneous reactivities of N₂O₅ and ClONO₂ on the TiO₂ and SiO₂ surface at the molecular level cannot be derived from our data.

4.4 Comparison with previous work

We find that, in the absence of HCl, $\gamma(\text{ClONO}_2)$ is around 1.2×10^{-3} for TiO₂ aerosol particles and $< 1 \times 10^{-3}$ for SiO₂ aerosol particles at room temperature. Using the coated-wall flow tube technique, Molina et al. (1997) investigated the uptake of ClONO₂ onto the inner wall of an Al₂O₃ tube, α -Al₂O₃ particles and the inner wall of a Pyrex glass tube, in the presence of $(1-10) \times 10^{-6}$ torr HCl at 200–220 K. Uptake coefficients of ~ 0.02 were reported for all the three types of surface (including Pyrex glass), over a factor of 1000 larger than $\gamma(\text{ClONO}_2)$ for Pyrex glass determined in our present work. The large difference in $\gamma(\text{ClONO}_2)$ reported by the two studies is likely due to the co-presence of HCl (1×10^{-6} – 1×10^{-5} torr) in the experiments of Molina et al. (1997), while no HCl was present in our work. Heterogeneous reactions of ClONO₂ proceed via direct and acid-catalysed hydrolysis (Robinson et al., 1997; Shi et al., 2001; Ammann et al., 2013), and numerous previous studies have confirmed that the presence of HCl in the gas phase (and thus partitioning into or adsorption onto the condensed phases) promotes the uptake of ClONO₂ by H₂SO₄ solution, ice and NAT, as summarised by Crowley et al. (2010), Burkholder et al. (2015) and Ammann et al. (2013). Temperature may also play a role since measurements were carried out at 200–220 K by Molina et al. (1997) and at ~ 296 K in our study.

Considering the importance of HCl in the ClONO₂ uptake and its abundance in the stratosphere, it will be important to systematically measure $\gamma(\text{ClONO}_2)$ for SiO₂/TiO₂ in the presence of HCl over a broad HCl concentration and temperature range relevant for the lower stratosphere.

5 Implication for stratospheric particle injection

Injection of TiO₂ into the stratosphere will provide additional surface area for the heterogeneous reactions of N₂O₅ (Reaction R1a) and ClONO₂ (Reactions R1b, R1c). There are several important types of particles naturally present in the stratosphere (Solomon, 1999), including sulfuric acid, ice and NAT, and their interaction with ClONO₂ has been well characterised (Crowley et al., 2010; Ammann et al., 2013; Burkholder et al., 2015). Comparing $\gamma(\text{ClONO}_2)$ for TiO₂ particles with these other stratospherically relevant surfaces can provide a first-order estimate of their relative importance.

The uptake of ClONO₂ on H₂SO₄ acid particles is strongly influenced by temperature and the water content in the particles (Shi et al., 2001; Ammann et al., 2013; Burkholder et al., 2015): $\gamma(\text{ClONO}_2)$ are $< 2 \times 10^{-3}$ for 65 wt % H₂SO₄ particles and $< 2 \times 10^{-4}$ for 75 wt % H₂SO₄ particles. The global distribution of $\gamma(\text{ClONO}_2)$ calculated for sulfuric acid particles in the stratosphere is shown in the Supplement (Fig. S3), suggesting that $\gamma(\text{ClONO}_2)$ is lower on TiO₂ particles than on sulfuric acid particles in the lower stratosphere. The uptake coefficient of ClONO₂ for water ice shows a negative dependence on temperature, with $\gamma(\text{ClONO}_2)$ of ~ 0.1 at ~ 200 K (Crowley et al., 2010; Burkholder et al., 2015), around a factor of 100 larger than that for TiO₂ particles at room temperature. $\gamma(\text{ClONO}_2)$ for water-rich nitric acid trihydrate (NAT), another important component for polar stratospheric clouds, increases strongly with temperature, with $\gamma(\text{ClONO}_2)$ of 3.0×10^{-3} at 200 K, 6.0×10^{-3} at 210 K and 1.14×10^{-2} at 220 K (Crowley et al., 2010).

While the background burden of stratospheric aerosol is low, volcanic eruptions and deliberate stratospheric particle injection for climate engineering purposes have the potential to significantly increase the available surfaces for heterogeneous reactions. In our current work, three simulations were performed, one representing a low background loading of stratospheric sulfate (< 1 Tg) aerosols (S1), a second representing the eruption of Mt Pinatubo (S2) and a third representing an instantaneous injection of 10 Tg of TiO₂ (S3). SiO₂ particle injection is not considered in our modelling study because the refractive index of SiO₂ is significantly smaller than TiO₂ (Pope et al., 2012). Two heterogeneous reactions on TiO₂ particles, i.e. heterogeneous hydrolysis of N₂O₅ (Reaction R1a) and ClONO₂ (Reaction R1b), were included in the simulation: a value of 1.5×10^{-3} was used for $\gamma(\text{N}_2\text{O}_5)$, as measured in our previous work (Tang et al., 2014c), and $\gamma(\text{ClONO}_2)$ was also set to 1.5×10^{-3} , based on the measurement reported in our current study. All three simulations were nudged to observed meteorology from December 1990 to January 1993. By comparing the TiO₂ injection (S3) with the Mt Pinatubo eruption (S2), we are able to quantify the relative impacts of TiO₂ and sulfuric acid injection on stratospheric chemistry. Results in this section are presented as annual means for the year 1992.

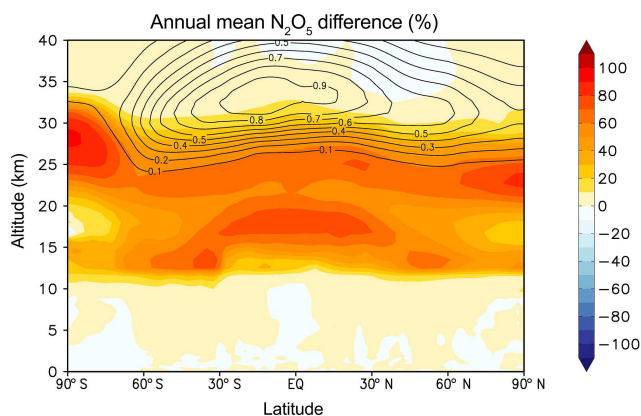


Figure 6. Simulated annual-mean, zonal-mean N₂O₅ percentage differences between TiO₂ injection (S3) and the Mt Pinatubo eruption (S2). Black contour lines show N₂O₅ mixing ratios from the Mt Pinatubo simulation (S2) in ppbv.

Similar to our previous study (Tang et al., 2014c), we have found that injection of TiO₂ (S3) has a much smaller impact on stratospheric N₂O₅ concentrations than the eruption of Mt Pinatubo (S2). N₂O₅ mixing ratios are significantly reduced in S2 compared to S1 from 10 to 30 km, with concentrations reduced by > 80 % throughout most of this region. For comparison, after TiO₂ injection (S3) N₂O₅ concentrations are reduced over a much smaller altitude range (15–25 km) and to a lesser degree, with ~ 20 % reductions in the tropics and up to 60 % reductions in the high latitudes. The relative effects of TiO₂ injection compared to sulfate injection on N₂O₅ mixing ratios is calculated as the difference between S3 and S2. As shown in Fig. 6, throughout most of the stratosphere N₂O₅ mixing ratios remain higher under S3 than S2.

Under both particle injection scenarios (S2 and S3), stratospheric ClO_x mixing ratios are increased compared to S1 due to the activation of ClONO₂ through heterogeneous reactions. However, Fig. 7 suggests that ClO_x mixing ratios are up to 40 % lower in the tropical lower stratosphere following the injection of TiO₂ aerosols compared to sulfate. This is driven in part by the lower surface area density of TiO₂ compared to sulfate but is also due to the difference in uptake coefficients. The uptake coefficient of ClONO₂ onto sulfate is temperature-dependent, and our measurements suggest that the uptake coefficient onto fresh TiO₂ is smaller than that for sulfate below ~ 215 K. Throughout much of the tropical lower stratosphere where maximum aerosol surface area density is found in both S2 and S3, temperatures are below ~ 220 K, and therefore the uptake coefficient is lower for TiO₂ than sulfate (as shown by Fig. S3 in the Supplement), leading to reduced chlorine activation. Previous studies have investigated the influence of temperature on the heterogeneous reactions of mineral particles with a few other trace gases – including HCOOH (Wu et al., 2012), H₂O₂

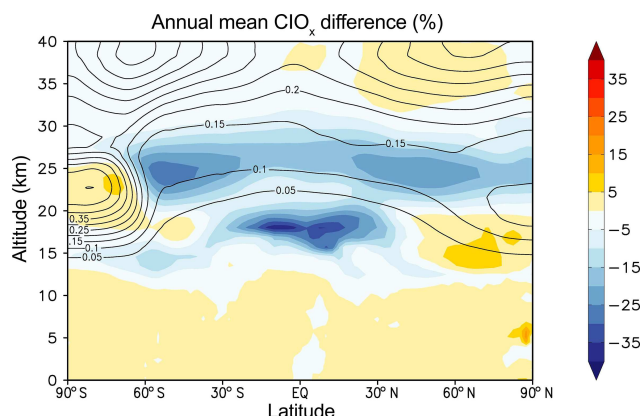


Figure 7. Simulated annual-mean, zonal-mean ClO_x percentage differences between TiO₂ injection (S3) and the Mt Pinatubo eruption (S2). Black contour lines show ClO_x mixing ratios from the Mt Pinatubo simulation (S2) in ppbv.

(Romanias et al., 2012) and OH radicals (Bedjanian et al., 2013) – and found that the measured uptake coefficients varied only by a factor of 2–3 or less across a wide temperature range. However, it is unclear whether temperature would have a significant effect on $\gamma(\text{ClONO}_2)$ for TiO₂ particles, and therefore our simulated impact of heterogeneous reaction of ClONO₂ with TiO₂ on stratospheric chemistry may have large uncertainties. The sensitivity of simulated stratospheric compositions to $\gamma(\text{ClONO}_2)$ for TiO₂ particles will be investigated in a following paper.

The relative difference in ozone mixing ratios following TiO₂ injection (S3) compared with the eruption of Mt Pinatubo (S2) is shown in Fig. 8. Ozone mixing ratios in the lower stratosphere decrease as a result of both TiO₂ and sulfate injection, with the largest decreases seen at high latitudes. In terms of annual means, the magnitude of this ozone response is comparable between the two simulations, with a maximum of ~ 3 % in the tropics and ~ 7 % at high latitudes. In contrast, ozone mixing ratios at the altitude of 25 km increase following the eruption of Mt Pinatubo (S2) but show no significant change upon TiO₂ injection (S3). This is consistent with the much faster uptake of N₂O₅ onto sulfate aerosols and the resultant stratospheric NO_x loss and decreases in the rates of catalytic ozone destruction at these altitudes.

The results presented here indicate that there is little difference in stratospheric ozone concentrations between injection of TiO₂ and sulfate aerosols when Reactions (R1a) and (R1b) are considered on TiO₂. While TiO₂ injection (S3) leads to less ClO_x activation and ozone destruction in the lowermost stratosphere, the reduced depletion of N₂O₅ and NO_x in the middle stratosphere leads to decreased ozone mixing ratios compared to sulfate injection (S2). The total column ozone differences between S3 and S2 are within ±2.5 %, indicating that there is no significant difference in vertically integrated

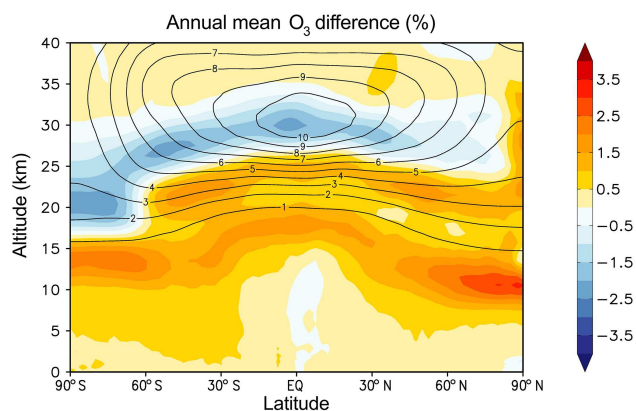


Figure 8. Simulated annual-mean, zonal-mean O₃ percentage differences between TiO₂ injection (S3) and the Mt Pinatubo eruption (S2). Black contour lines show ClO_x mixing ratios from the Mt Pinatubo simulation (S2) in parts per million by volume (ppmv).

ozone abundances and solar UV amounts reaching the surface. However, more work is required to establish additional kinetic data for heterogeneous reactions of TiO₂.

6 Conclusions and outlook

Minerals with high refractive indices, such as TiO₂, have been proposed as possible materials used for stratospheric particle injection for climate engineering (Pope et al., 2012). However, kinetic data of their heterogeneous reactions with important reactive trace gases (e.g. N₂O₅ and ClONO₂) in the stratosphere are lacking, impeding us from a reliable assessment of the impacts of mineral particle injection on stratospheric ozone in particular and stratosphere chemistry in general. In our current work, using an atmospheric pressure aerosol flow tube, we have investigated the heterogeneous reaction of ClONO₂ with TiO₂ and SiO₂ aerosol particles at room temperature and at different RHs. The uptake coefficient, $\gamma(\text{ClONO}_2)$, was $\sim 1.2 \times 10^{-3}$ at 7 and 33 % RH for TiO₂ particles, with no significant difference observed at these two RHs; for SiO₂ particles, $\gamma(\text{ClONO}_2)$ increases from $\sim 2 \times 10^{-4}$ at 7 % RH to $\sim 6 \times 10^{-4}$ at 59 % RH, showing a positive dependence on RH. Therefore, it can be concluded that, under similar conditions for the RH range covered in this work, TiO₂ shows higher heterogeneous reactivity than SiO₂ towards ClONO₂. Compared to sulfuric acid particles in the lower stratosphere, the heterogeneous reactivity towards ClONO₂ is lower for TiO₂ particles. In addition, the heterogeneous uptake of ClONO₂ by Pyrex glass was also studied, with $\gamma(\text{ClONO}_2)$ increasing from $\sim 4.5 \times 10^{-6}$ at 0 % RH to $\sim 1.6 \times 10^{-5}$ at 24 % RH.

Using the UKCA chemistry–climate model with nudged meteorology, we have constructed a scenario to assess the impact of TiO₂ particle injection on stratospheric chemistry. In this scenario TiO₂ aerosol particles are distributed in the stratosphere in such a way that TiO₂ particle injection is expected to produce a radiative effect similar to that of the Mt Pinatubo eruption, following Pope et al. (2012). Heterogeneous reactions of N₂O₅ and ClONO₂ with TiO₂ aerosol particles, both with an uptake coefficient of 1.5×10^{-3} based on our previous (Tang et al., 2014c) and current laboratory experiments, were included in the simulation. It is found that, compared to the eruption of Mt Pinatubo, the TiO₂ injection has a much smaller impact on N₂O₅ in the stratosphere, although significant reduction (20–60 % compared to the background scenario without additional particle injection) in stratospheric N₂O₅ also occurs. Compared to the background scenario, both TiO₂ injection and the Mt Pinatubo eruption scenarios lead to increased stratospheric ClO_x mixing ratios, and the ClO_x mixing ratios are lower for the TiO₂ injection than the Mt Pinatubo eruption. Both TiO₂ injection and the Mt Pinatubo eruption result in significant ozone depletion in the lower stratosphere, with the largest decreases occurring at high latitudes. In comparison with Mt Pinatubo eruption, TiO₂ injection causes less ClO_x activation and less ozone destruction in the lowermost stratosphere, while the reduced depletion of N₂O₅ and NO_x in the middle stratosphere results in decreased ozone levels. Overall, our simulation results suggest that there is no significant difference (within ± 2.5 %) in the vertically integrated ozone abundances between TiO₂ injection and Mt Pinatubo eruption.

It should be emphasised that heterogeneous chemistry of TiO₂ included in our current modelling study is not complete. One example is the heterogeneous reaction of ClONO₂ with HCl (Reaction R1c) on/in the particles. An uptake coefficient of 0.02 was reported for the heterogeneous reaction of ClONO₂ with HCl on Al₂O₃ particles (Molina et al., 1997), and it is reasonable to assume that this reaction may also be quite fast on TiO₂ particles. The heterogeneous reaction of ClONO₂ with HCl on TiO₂ particles, with an uptake coefficient assumed to be the same as that on the Al₂O₃ surface (i.e. 0.02) as reported by Molina et al. (1997), has been included in further simulations, and the results will be reported and discussed in a following paper. Other reactions, including the heterogeneous reaction of HOCl (Molina et al., 1996; Solomon, 1999) and a range of heterogeneous photochemical reactions (Chen et al., 2012; George et al., 2015), may also be important and thus deserve further laboratory and modelling investigation. In this work we have only considered heterogeneous chemistry of fresh TiO₂ particles. If injected into the stratosphere, TiO₂ particles would be coated with H₂SO₄, NAT, water ice etc., and heterogeneous reactivity of coated TiO₂ particles could be very different from fresh particles. This important issue should be addressed by further laboratory and modelling studies.

Our nudged modelling simulations, designed to focus on chemistry effects, do not take into account feedbacks between radiative effects, atmospheric dynamics and chemistry. Several recent studies have assessed the impact of high-latitude stratospheric ozone depletion using the UKCA model (Braesicke et al., 2013; Keeble et al., 2014) and have shown that interactive feedbacks can affect stratospheric temperatures, the strength of the Brewer–Dobson circulation, the longevity of polar vortices and surface climate. By nudging the model to observed meteorology during the Mt Pinatubo eruption, these feedbacks are implicitly included in the sulfate injection scenario. However, while we have chosen a TiO₂ loading to give the same surface radiative response as the Mt Pinatubo eruption, the stratospheric radiative impacts may differ. In order to fully understand the true impact of stratospheric particle injection, both the radiative and chemical effects, and the coupling between these responses, need to be explored further. In addition, before any climate engineering schemes could be considered, much consideration is absolutely obligatory, including, but not limited to, technical, socioeconomic, political, environmental and ethical feasibilities.

7 Data availability

The data used in this study are available from M. Tang (mingjintang@gig.ac.cn) and J. Keeble (jmk64@cam.ac.uk) upon request.

The Supplement related to this article is available online at doi:10.5194/acp-16-15397-2016-supplement.

Acknowledgements. Financial support provided by EPSRC grant EP/I01473X/1 and the Isaac Newton Trust (Trinity College, University of Cambridge, UK) is acknowledged. We thank NCAS-CMS for modelling support. Model integrations have been performed using the ARCHER UK National Supercomputing Service. We acknowledge the ERC for support through the ACCI project (project number: 267760). M. J. Tang would like to thank the CAS Pioneer Hundred Talents programme and State Key Laboratory of Organic Geochemistry for providing starting grants.

Edited by: V. F. McNeill

Reviewed by: two anonymous referees

References

Ammann, M., Cox, R. A., Crowley, J. N., Jenkin, M. E., Mellouki, A., Rossi, M. J., Troe, J., and Wallington, T. J.: Evaluated kinetic and photochemical data for atmospheric chemistry: Volume VI – heterogeneous reactions with liquid substrates, *Atmos. Chem. Phys.*, 13, 8045–8228, doi:10.5194/acp-13-8045-2013, 2013.

- Anderson, L. C. and Fahey, D. W.: Studies with ClONO₂: Thermal-dissociation rate and catalytic conversion to NO using an NO/O₃ chemi-luminescence detector, *J. Phys. Chem.*, 94, 644–652, 1990.
- Ball, S. M., Fried, A., Henry, B. E., and Mozurkewich, M.: The hydrolysis of ClONO₂ on sub-micron liquid sulfuric acid aerosol, *Geophys. Res. Lett.*, 25, 3339–3342, 1998.
- Ballard, J., Johnston, W. B., Gunson, M. R., and Wassell, P. T.: Absolute absorption coefficients of ClONO₂ infrared bands at stratospheric temperatures, *J. Geophys. Res.-Atmos.*, 93, 1659–1665, 1988.
- Bannan, T. J., Booth, A. M., Bacak, A., Muller, J. B. A., Leather, K. E., Le Breton, M., Jones, B., Young, D., Coe, H., Allan, J., Visser, S., Slowik, J. G., Furger, M., Prévôt, A. S. H., Lee, J., Dunmore, R. E., Hopkins, J. R., Hamilton, J. F., Lewis, A. C., Whalley, L. K., Sharp, T., Stone, D., Heard, D. E., Fleming, Z. L., Leigh, R., Shallcross, D. E., and Percival, C. J.: The first UK measurements of nitryl chloride using a chemical ionization mass spectrometer in central London in the summer of 2012, and an investigation of the role of Cl atom oxidation, *J. Geophys. Res.-Atmos.*, 120, 5638–5657, 2015.
- Bedjanian, Y., Romanias, M. N., and El Zein, A.: Interaction of OH Radicals with Arizona Test Dust: Uptake and Products, *J. Phys. Chem. A*, 117, 393–400, 2013.
- Braesicke, P., Keeble, J., Yang, X., Stiller, G., Kellmann, S., Abraham, N. L., Archibald, A., Telford, P., and Pyle, J. A.: Circulation anomalies in the Southern Hemisphere and ozone changes, *Atmos. Chem. Phys.*, 13, 10677–10688, doi:10.5194/acp-13-10677-2013, 2013.
- Brown, R. L.: Tubular flow reactors with first-order kinetics, *J. Res. Nat. Bur. Stand.*, 83, 1–8, 1978.
- Burkholder, J. B., Sander, S. P., Abbatt, J. P. D., Barker, J. R., Huie, R. E., Kolb, C. E., Kurylo, M. J., Orkin, V. L., Wilmouth, D. M., and Wine, P. H.: Chemical Kinetics and Photochemical Data for Use in Atmospheric Studies, Evaluation No. 18, JPL Publication 15-10, Jet Propulsion Lab., Pasadena, CA, 2015.
- Chen, H. H., Nanayakkara, C. E., and Grassian, V. H.: Titanium Dioxide Photocatalysis in Atmospheric Chemistry, *Chem. Rev.*, 112, 5919–5948, 2012.
- Chikazawa, M., Kanazawa, T., and Yamaguchi, T.: The Role of Adsorbed Water on Adhesion Force of Powder Particles, *KONA*, 2, 54–61, 1984.
- Chipperfield, M. P.: Multiannual simulations with a three-dimensional chemical transport model, *J. Geophys. Res.-Atmos.*, 104, 1781–1805, 1999.
- Crowley, J. N., Ammann, M., Cox, R. A., Hynes, R. G., Jenkin, M. E., Mellouki, A., Rossi, M. J., Troe, J., and Wallington, T. J.: Evaluated kinetic and photochemical data for atmospheric chemistry: Volume V – heterogeneous reactions on solid substrates, *Atmos. Chem. Phys.*, 10, 9059–9223, doi:10.5194/acp-10-9059-2010, 2010.
- Crutzen, P. J.: Albedo enhancement by stratospheric sulfur injections: A contribution to resolve a policy dilemma?, *Climatic Change*, 77, 211–219, 2006.
- Danilin, M. Y., Shia, R. L., Ko, M. K. W., Weisenstein, D. K., Sze, N. D., Lamb, J. J., Smith, T. W., Lohn, P. D., and Prather, M. J.: Global stratospheric effects of the alumina emissions by solid-fueled rocket motors, *J. Geophys. Res.-Atmos.*, 106, 12727–12738, 2001.

- Davidson, J. A., Cantrell, C. A., Shetter, R. E., McDaniel, A. H., and Calvert, J. G.: Absolute infrared absorption cross sections for ClONO₂ at 296 and 223 K, *J. Geophys. Res.-Atmos.*, 92, 10921–10925, 1987.
- Dee, D. P., Uppala, S. M., Simmons, A. J., Berrisford, P., Poli, P., Kobayashi, S., Andrae, U., Balmaseda, M. A., Balsamo, G., Bauer, P., Bechtold, P., Beljaars, A. C. M., van de Berg, L., Bidlot, J., Bormann, N., Delsol, C., Dragani, R., Fuentes, M., Geer, A. J., Haimberger, L., Healy, S. B., Hersbach, H., Holm, E. V., Isaksen, I., Kallberg, P., Kohler, M., Matricardi, M., McNally, A. P., Monge-Sanz, B. M., Morcrette, J. J., Park, B. K., Peubey, C., de Rosnay, P., Tavolato, C., Thepaut, J. N., and Vitart, F.: The ERA-Interim reanalysis: configuration and performance of the data assimilation system, *Q. J. Roy. Meteor. Soc.*, 137, 553–597, 2011.
- Deiber, G., George, Ch., Le Calvé, S., Schweitzer, F., and Mirabel, Ph.: Uptake study of ClONO₂ and BrONO₂ by Halide containing droplets, *Atmos. Chem. Phys.*, 4, 1291–1299, doi:10.5194/acp-4-1291-2004, 2004.
- Dutton, E. G., and Christy, J. R.: Solar radiative forcing at selected locations and evidence for global lower tropospheric cooling following the eruptions of El Chichón and Pinatubo, *Geophys. Res. Lett.*, 19, 2313–2316, 1992.
- Fahey, D. W., Eubank, C. S., Hubler, G., and Fehsenfeld, F. C.: A Calibrated Source of N₂O₅, *Atmos. Environ.*, 19, 1883–1890, 1985.
- Fahey, D. W., Kawa, S. R., Woodbridge, E. L., Tin, P., Wilson, J. C., Jonsson, H. H., Dye, J. E., Baumgardner, D., Borrmann, S., Toohey, D. W., Avallone, L. M., Proffitt, M. H., Margitan, J., Loewenstein, M., Podolske, J. R., Salawitch, R. J., Wofsy, S. C., Ko, M. K. W., Anderson, D. E., Schoeberl, M. R., and Chan, K. R.: In situ measurement constraining the role of sulfate aerosol in midlatitude ozone depletion, *Nature*, 363, 509–514, 1993.
- Fernandez, M. A., Hynes, R. G., and Cox, R. A.: Kinetics of ClONO₂ reactive uptake on ice surfaces at temperatures of the upper troposphere, *J. Phys. Chem. A*, 109, 9986–9996, 2005.
- Ferraro, A. J., Highwood, E. J., and Charlton-Perez, A. J.: Stratospheric heating by potential geoengineering aerosols, *Geophys. Res. Lett.*, 38, L24706, doi:10.1029/2011GL049761, 2011.
- Finlayson-Pitts, B. J., Ezell, M. J., and Pitts, J. N.: Formation of Chemically Active Chlorine Compounds by Reactions of Atmospheric NaCl Particles with Gaseous N₂O₅ and ClONO₂, *Nature*, 337, 241–244, 1989.
- George, C., Ammann, M., D’Anna, B., Donaldson, D. J., and Nizkorodov, S. A.: Heterogeneous Photochemistry in the Atmosphere, *Chem. Rev.*, 115, 4218–4258, 2015.
- Ginoux, P., Prospero, J. M., Gill, T. E., Hsu, N. C., and Zhao, M.: Global-scale Attribution of Anthropogenic and Natural Dust Sources and Their Emission Rates Based on MODIS Deep Blue Aerosol Products, *Rev. Geophys.*, 50, RG3005, doi:10.1029/2012RG000388, 2012.
- Goodman, A. L., Bernard, E. T., and Grassian, V. H.: Spectroscopic Study of Nitric Acid and Water Adsorption on Oxide Particles: Enhanced Nitric Acid Uptake Kinetics in the Presence of Adsorbed Water, *J. Phys. Chem. A*, 105, 6443–6457, 2001.
- Guo, S., Bluth, G. J. S., Rose, W. I., Watson, I. M., and Prata, A. J.: Re-evaluation of SO₂ release of the 15 June 1991 Pinatubo eruption using ultraviolet and infrared satellite sensors, *Geochem. Geophys. Geosys.*, 5, Q04001, doi:10.1029/2003GC000654, 2004.
- Hanson, D. R.: Reaction of ClONO₂ with H₂O and HCl in sulfuric acid and HNO₃/H₂SO₄/H₂O mixtures, *J. Phys. Chem. A*, 102, 4794–4807, 1998.
- Hanson, D. R. and Lovejoy, E. R.: The Reaction of ClONO₂ with Submicrometer Sulfuric-Acid Aerosol, *Science*, 267, 1326–1328, 1995.
- Hanson, D. R. and Ravishankara, A. R.: The reaction probabilities of ClONO₂ and N₂O₅ on polar stratospheric cloud materials, *J. Geophys. Res.-Atmos.*, 96, 5081–5090, 1991.
- Hanson, D. R. and Ravishankara, A. R.: Reactive uptake of ClONO₂ onto sulfuric-acid due to reaction with HCl and H₂O, *J. Phys. Chem.*, 98, 5728–5735, 1994.
- Hauglustaine, D. A., Hourdin, F., Jourdain, L., Filiberti, M. A., Walters, S., Lamarque, J. F., and Holland, E. A.: Interactive chemistry in the Laboratoire de Meteorologie Dynamique general circulation model: Description and background tropospheric chemistry evaluation, *J. Geophys. Res.-Atmos.*, 109, D04314, doi:10.1029/2003JD003957, 2004.
- Hinds, W. C.: Aerosol techniques: properties, behavior, and measurement of airborne particles, John Wiley & Sons, Inc., New York, 1996.
- Howard, C. J.: Kinetic Measurements Using Flow Tubes, *J. Phys. Chem.*, 83, 3–9, 1979.
- Jackman, C. H., Considine, D. B., and Fleming, E. L.: A global modeling study of solid rocket aluminum oxide emission effects on stratospheric ozone, *Geophys. Res. Lett.*, 25, 907–910, 1998.
- Jeuken, A. B. M., Siegmund, P. C., Heijboer, L. C., Feichter, J., and Bengtsson, L.: On the potential of assimilating meteorological analyses in a global climate model for the purpose of model validation, *J. Geophys. Res.-Atmos.*, 101, 16939–16950, 1996.
- Jones, A. C., Haywood, J. M., and Jones, A.: Climatic impacts of stratospheric geoengineering with sulfate, black carbon and titanium injection, *Atmos. Chem. Phys.*, 16, 2843–2862, 2016.
- Kebede, M. A., Scharko, N. K., Appelt, L. E., and Raff, J. D.: Formation of Nitrous Acid during Ammonia Photooxidation on TiO₂ under Atmospherically Relevant Conditions, *J. Phys. Chem. Lett.*, 4, 2618–2623, 2013.
- Keeble, J., Braesicke, P., Abraham, N. L., Roscoe, H. K., and Pyle, J. A.: The impact of polar stratospheric ozone loss on Southern Hemisphere stratospheric circulation and climate, *Atmos. Chem. Phys.*, 14, 13705–13717, doi:10.5194/acp-14-13705-2014, 2014.
- Kravitz, B., Robock, A., Forster, P. M., Haywood, J. M., Lawrence, M. G., and Schmidt, H.: An overview of the Geoengineering Model Intercomparison Project (GeoMIP), *J. Geophys. Res.-Atmos.*, 118, 13103–13107, 2013.
- Lawler, M. J., Sander, R., Carpenter, L. J., Lee, J. D., von Glasow, R., Sommariva, R., and Saltzman, E. S.: HOCl and Cl₂ observations in marine air, *Atmos. Chem. Phys.*, 11, 7617–7628, doi:10.5194/acp-11-7617-2011, 2011.
- Lee, S. H., Leard, D. C., Zhang, R. Y., Molina, L. T., and Molina, M. J.: The HCl + ClONO₂ reaction rate on various water ice surfaces, *Chem. Phys. Lett.*, 315, 7–11, 1999.
- Liao, J., Huey, L. G., Liu, Z., Tanner, D. J., Cantrell, C. A., Orlando, J. J., Flocke, F. M., Shepson, P. B., Weinheimer, A. J., Hall, S. R., Ullmann, K., Beine, H. J., Wang, Y., Ingall, E. D., Stephens, C. R., Hornbrook, R. S., Apel, E. C., Riemer, D., Fried, A., Mauldin III, R. L., Smith, J. N., Staebler, R. M., Neuman, J.

- A., and Nowak, J. B.: High levels of molecular chlorine in the Arctic atmosphere, *Nat. Geosci.*, 7, 91–94, 2014.
- McCormick, M. P., Thomason, L. W., and Trepte, C. R.: Atmospheric effects of the Mt Pinatubo eruption, *Nature*, 373, 399–404, 1995.
- Molina, L. T., Spencer, J. E., and Molina, M. J.: The rate constant for the reaction of O(³P) atoms with ClONO₂, *Chem. Phys. Lett.*, 45, 158–162, 1977.
- Molina, M. J., Molina, L. T., and Kolb, C. E.: Gas-phase and heterogeneous chemical kinetics of the troposphere and stratosphere, *Annu. Rev. Phys. Chem.*, 47, 327–367, 1996.
- Molina, M. J., Molina, L. T., Zhang, R. Y., Meads, R. F., and Spencer, D. D.: The reaction of ClONO₂ with HCl on aluminum oxide, *Geophys. Res. Lett.*, 24, 1619–1622, 1997.
- Morgenstern, O., Braesicke, P., O'Connor, F. M., Bushell, A. C., Johnson, C. E., Osprey, S. M., and Pyle, J. A.: Evaluation of the new UKCA climate-composition model – Part 1: The stratosphere, *Geosci. Model Dev.*, 2, 43–57, doi:10.5194/gmd-2-43-2009, 2009.
- O'Connor, F. M., Johnson, C. E., Morgenstern, O., Abraham, N. L., Braesicke, P., Dalvi, M., Folberth, G. A., Sanderson, M. G., Telford, P. J., Voulgarakis, A., Young, P. J., Zeng, G., Collins, W. J., and Pyle, J. A.: Evaluation of the new UKCA climate-composition model – Part 2: The Troposphere, *Geosci. Model Dev.*, 7, 41–91, doi:10.5194/gmd-7-41-2014, 2014.
- Osthoff, H. D., Roberts, J. M., Ravishankara, A. R., Williams, E. J., Lerner, B. M., Sommariva, R., Bates, T. S., Coffman, D., Quinn, P. K., Dibb, J. E., Stark, H., Burkholder, J. B., Talukdar, R. K., Meagher, J., Fehsenfeld, F. C., and Brown, S. S.: High levels of nitryl chloride in the polluted subtropical marine boundary layer, *Nat. Geosci.*, 1, 324–328, 2008.
- Phillips, G. J., Tang, M. J., Thieser, J., Brickwedde, B., Schuster, G., Bohn, B., Lelieveld, J., and Crowley, J. N.: Significant concentrations of nitryl chloride observed in rural continental Europe associated with the influence of sea salt chloride and anthropogenic emissions, *Geophys. Res. Lett.*, 39, L10811, doi:10.1029/2012gl051912, 2012.
- Pope, F. D., Braesicke, P., Grainger, R. G., Kalberer, M., Watson, I. M., Davidson, P. J., and Cox, R. A.: Stratospheric aerosol particles and solar-radiation management, *Nat. Clim. Change*, 2, 713–719, 2012.
- Renard, J. J. and Bolker, H. I.: The chemistry of chlorine monoxide (dichlorine monoxide), *Chem. Rev.*, 76, 487–508, 1976.
- Riedel, T. P., Bertram, T. H., Crisp, T. A., Williams, E. J., Lerner, B. M., Vlasenko, A., Li, S.-M., Gilman, J., de Gouw, J., Bon, D. M., Wagner, N. L., Brown, S. S., and Thornton, J. A.: Nitryl Chloride and Molecular Chlorine in the Coastal Marine Boundary Layer, *Environ. Sci. Technol.*, 46, 10463–10470, 2012.
- Robinson, G. N., Worsnop, D. R., Jayne, J. T., Kolb, C. E., and Davidovits, P.: Heterogeneous uptake of ClONO₂ and N₂O₅ by sulfuric acid solutions, *J. Geophys. Res.-Atmos.*, 102, 3583–3601, 1997.
- Romanias, M. N., El Zein, A., and Bedjanian, Y.: Heterogeneous Interaction of H₂O₂ with TiO₂ Surface under Dark and UV Light Irradiation Conditions, *J. Phys. Chem. A*, 116, 8191–8200, 2012.
- Rouviere, A., Sosedova, Y., and Ammann, M.: Uptake of Ozone to Deliquesced KI and Mixed KI/NaCl Aerosol Particles, *J. Phys. Chem. A*, 114, 7085–7093, 2010.
- Schack, C. J. and Lindahl, C. B.: On the synthesis of chlorine monoxide, *Inorg. Nucl. Chem. Lett.*, 3, 387–389, 1967.
- Schmidt, G. A., Ruedy, R., Hansen, J. E., Aleinov, I., Bell, N., Bauer, M., Bauer, S., Cairns, B., Canuto, V., Cheng, Y., Del Genio, A., Faluvegi, G., Friend, A. D., Hall, T. M., Hu, Y. Y., Kelley, M., Kiang, N. Y., Koch, D., Lacis, A. A., Lerner, J., Lo, K. K., Miller, R. L., Nazarenko, L., Oinas, V., Perlwitz, J., Perlwitz, J., Rind, D., Romanou, A., Russell, G. L., Sato, M., Shindell, D. T., Stone, P. H., Sun, S., Tausnev, N., Thresher, D., and Yao, M. S.: Present-day atmospheric simulations using GISS ModelE: Comparison to in situ, satellite, and reanalysis data, *J. Climate*, 19, 153–192, 2006.
- Shang, J., Li, J., and Zhu, T.: Heterogeneous Reaction of SO₂ on TiO₂ Particles, *Sci. China Chem.*, 53, 2637–2643, 2010.
- Shepherd, J.: *Geoengineering the climate: science, governance and uncertainty*, The Royal Society, London, UK, 2009.
- Shi, Q., Jayne, J. T., Kolb, C. E., Worsnop, D. R., and Davidovits, P.: Kinetic model for reaction of ClONO₂ with H₂O and HCl and HOCl with HCl in sulfuric acid solutions, *J. Geophys. Res.-Atmos.*, 106, 24259–24274, 2001.
- Simpson, W. R., Brown, S. S., Saiz-Lopez, A., Thornton, J. A., and v. Glasow, R.: *Tropospheric Halogen Chemistry: Sources, Cycling, and Impacts*, *Chem. Rev.*, 115, 4035–4062, 2015.
- Solomon, S.: Stratospheric ozone depletion: A review of concepts and history, *Rev. Geophys.*, 37, 275–316, 1999.
- SPARC: *Assessment of Stratospheric Aerosol Properties (SPARC Report No. 4)*, 2006.
- Spicer, C. W., Chapman, E. G., Finlayson-Pitts, B. J., Plastringe, R. A., Hubbe, J. M., Fast, J. D., and Berkowitz, C. M.: Unexpectedly high concentrations of molecular chlorine in coastal air, *Nature*, 394, 353–356, 1998.
- Stull, D. R.: *Vapor Pressure of Pure Substances. Organic and Inorganic Compounds*, *Ind. Eng. Chem.*, 39, 517–540, 1947.
- Takemura, T., Okamoto, H., Maruyama, Y., Numaguti, A., Higurashi, A., and Nakajima, T.: Global three-dimensional simulation of aerosol optical thickness distribution of various origins, *J. Geophys. Res.-Atmos.*, 105, 17853–17873, 2000.
- Tang, M. J., Thieser, J., Schuster, G., and Crowley, J. N.: Kinetics and Mechanism of the Heterogeneous Reaction of N₂O₅ with Mineral Dust Particles, *Phys. Chem. Chem. Phys.*, 14, 8551–8561, 2012.
- Tang, M. J., Camp, J. C. J., Rkiouak, L., McGregor, J., Watson, I. M., Cox, R. A., Kalberer, M., Ward, A. D., and Pope, F. D.: Heterogeneous Interaction of SiO₂ with N₂O₅: Aerosol Flow Tube and Single Particle Optical Levitation-Raman Spectroscopy Studies, *J. Phys. Chem. A*, 118, 8817–8827, 2014a.
- Tang, M. J., Cox, R. A., and Kalberer, M.: Compilation and evaluation of gas phase diffusion coefficients of reactive trace gases in the atmosphere: volume 1. Inorganic compounds, *Atmos. Chem. Phys.*, 14, 9233–9247, doi:10.5194/acp-14-9233-2014, 2014b.
- Tang, M. J., Telford, P. J., Pope, F. D., Rkiouak, L., Abraham, N. L., Archibald, A. T., Braesicke, P., Pyle, J. A., McGregor, J., Watson, I. M., Cox, R. A., and Kalberer, M.: Heterogeneous reaction of N₂O₅ with airborne TiO₂ particles and its implication for stratospheric particle injection, *Atmos. Chem. Phys.*, 14, 6035–6048, doi:10.5194/acp-14-6035-2014, 2014c.
- Tang, M. J., Cziczo, D. J., and Grassian, V. H.: Interactions of Water with Mineral Dust Aerosol: Water Adsorption, Hygroscopicity,

- Cloud Condensation and Ice Nucleation, *Chem. Rev.*, 116, 4205–4259, 2016.
- Telford, P., Braesicke, P., Morgenstern, O., and Pyle, J.: Reassessment of causes of ozone column variability following the eruption of Mount Pinatubo using a nudged CCM, *Atmos. Chem. Phys.*, 9, 4251–4260, doi:10.5194/acp-9-4251-2009, 2009.
- Telford, P. J., Braesicke, P., Morgenstern, O., and Pyle, J. A.: Technical Note: Description and assessment of a nudged version of the new dynamics Unified Model, *Atmos. Chem. Phys.*, 8, 1701–1712, doi:10.5194/acp-8-1701-2008, 2008.
- Textor, C., Schulz, M., Guibert, S., Kinne, S., Balkanski, Y., Bauer, S., Bernsten, T., Berglen, T., Boucher, O., Chin, M., Dentener, F., Diehl, T., Easter, R., Feichter, H., Fillmore, D., Ghan, S., Ginoux, P., Gong, S., Grini, A., Hendricks, J., Horowitz, L., Huang, P., Isaksen, I., Iversen, I., Kloster, S., Koch, D., Kirkevåg, A., Kristjansson, J. E., Krol, M., Lauer, A., Lamarque, J. F., Liu, X., Montanaro, V., Myhre, G., Penner, J., Pitari, G., Reddy, S., Seland, Ø., Stier, P., Takemura, T., and Tie, X.: Analysis and quantification of the diversities of aerosol life cycles within AeroCom, *Atmos. Chem. Phys.*, 6, 1777–1813, doi:10.5194/acp-6-1777-2006, 2006.
- Thornton, J. A., Kercher, J. P., Riedel, T. P., Wagner, N. L., Cozic, J., Holloway, J. S., Dube, W. P., Wolfe, G. M., Quinn, P. K., Middlebrook, A. M., Alexander, B., and Brown, S. S.: A large atomic chlorine source inferred from mid-continental reactive nitrogen chemistry, *Nature*, 464, 271–174, 2010.
- Tilmes, S., Muller, R., and Salawitch, R.: The sensitivity of polar ozone depletion to proposed geoengineering schemes, *Science*, 320, 1201–1204, 2008.
- Tilmes, S., Mills, M. J., Niemeier, U., Schmidt, H., Robock, A., Kravitz, B., Lamarque, J.-F., Pitari, G., and English, J. M.: A new Geoengineering Model Intercomparison Project (GeoMIP) experiment designed for climate and chemistry models, *Geosci. Model Dev.*, 8, 43–49, doi:10.5194/gmd-8-43-2015, 2015.
- Wagner, C., Hanisch, F., Holmes, N., de Coninck, H., Schuster, G., and Crowley, J. N.: The interaction of N₂O₅ with mineral dust: aerosol flow tube and Knudsen reactor studies, *Atmos. Chem. Phys.*, 8, 91–109, doi:10.5194/acp-8-91-2008, 2008.
- Wang, T., Tham, Y. J., Xue, L., Li, Q., Zha, Q., Wang, Z., Poon, S. C. N., Dubé, W. P., Blake, D. R., Louie, P. K. K., Luk, C. W. Y., Tsui, W., and Brown, S. S.: Observations of nitryl chloride and modeling its source and effect on ozone in the planetary boundary layer of southern China, *J. Geophys. Res.-Atmos.*, 121, 2476–2489, 2016.
- Weisenstein, D. K., Keith, D. W., and Dykema, J. A.: Solar geoengineering using solid aerosol in the stratosphere, *Atmos. Chem. Phys.*, 15, 11835–11859, doi:10.5194/acp-15-11835-2015, 2015.
- Wilson, J. C., Jonsson, H. H., Brock, C. A., Toohey, D. W., Avalone, L. M., Baumgardner, D., Dye, J. E., Poole, L. R., Woods, D. C., Decoursey, R. J., Osborn, M., Pitts, M. C., Kelly, K. K., Chan, K. R., Ferry, G. V., Loewenstein, M., Podolske, J. R., and Weaver, A.: In-situ observations of aerosol and chlorine monoxide after the 1991 eruption of Mount-Pinatubo: effect of reactions on sulfate aerosol, *Science*, 261, 1140–1143, 1993.
- Wu, L.-Y., Tong, S.-R., Hou, S.-Q., and Ge, M.-F.: Influence of Temperature on the Heterogeneous Reaction of Formic Acid on α -Al₂O₃, *J. Phys. Chem. A*, 116, 10390–10396, 2012.
- Zhang, R. Y., Jayne, J. T., and Molina, M. J.: Heterogeneous interactions of ClONO₂ and HCl with sulfuric acid tetrahydrate: implications for the stratosphere, *J. Phys. Chem.*, 98, 867–874, 1994.